Simulation Validation for a Unmanned Semi-Submersible Vehicle

L.J. Larkin, C.J. Thomsen
Perry Technologies
Lockheed Martin Naval Electronics & Surveillance Systems
100 E. 17th Street
Riviera Beach, FL 33404

Abstract - Unmanned systems are a key component in the U.S. Navy's plan to reduce operational costs, increase operational effectiveness and reduce human exposure in high-risk environments. A key program for this pursuit is the AN/WLD-1(V)1 Remote Minehunting System. A major component of this system is the Remote Minehunting Vehicle (RMV), an unmanned semi-submersible which provides propulsion, guidance and control, and communications while towing the AN/AQS-20X Variable Depth Sensor (VDS) system.

I. INTRODUCTION

In order to provide mine reconnaissance capability over a wide variety of water depths and sea state conditions, stringent vehicle motion requirements were imposed on the RMV. A high fidelity simulation of the RMV, the VDS and the interconnecting tow cable was created for the purpose of control system development and performance verification. A real-time implementation of the simulation is used for software development and operator training.

Validation of the simulation was accomplished by at-sea testing of prototype vehicles. Configuration differences between the prototype vehicle and the production vehicle were accounted for in assessing the prototype test results. Production system risk is significantly reduced due to the excellent agreement between the simulation and the sea trial data.

A. Nomenclature

X Hydrodynamic force component along x-axis.

Y Hydrodynamic force component along y-axis.

Z Hydrodynamic force component along z-axis.

K Hydrodynamic moment component about x-axis.

M Hydrodynamic moment component about y-axis.

N Hydrodynamic moment component about z-axis.

ϕ Angle of roll.

θ Angle of pitch.

ψ Angle of yaw.

p Angular velocity about x-axis (roll rate).

q Angular velocity about y-axis (pitch rate).

r Angular velocity about z-axis (yaw rate).

U Velocity of origin of body axes relative to fluid.

u Component of U in the direction of the x-axis.

v Component of U in the direction of the y-axis.

w Component of U in the direction of the z-axis.

l Length of vehicle.

m Mass of vehicle.

B. System Description

The Remote Minehunting System (RMS) consists of a Remote Minehunting Vehicle (RMV), a Variable Depth Sonar (VDS) and an on-board Remote Minehunting Functional Segment (RMFS). This system has been designated AN/WLD-1(V)1 by the U.S. Navy. The U.S. Navy will deploy the AN/WLD-1(V)1 in 2005 on a select number of Arleigh Burke Class Flight IIA destroyers. Fig. 1 shows the RMS.

Fueled for long endurance, the RMV's 370 hp Cummins diesel marine engine and high-efficiency, torque balanced propulsor can drive the 23-ft.-long (7m) vehicle at speeds exceeding 16 knots. A streamlined snorkel/mast--the vehicle's only visible feature above the waterline--draws air into the engine, and provides a platform for RF antennas and an obstacle avoidance video camera. The nose module features a forward-looking sonar for detection and avoidance of underwater objects.

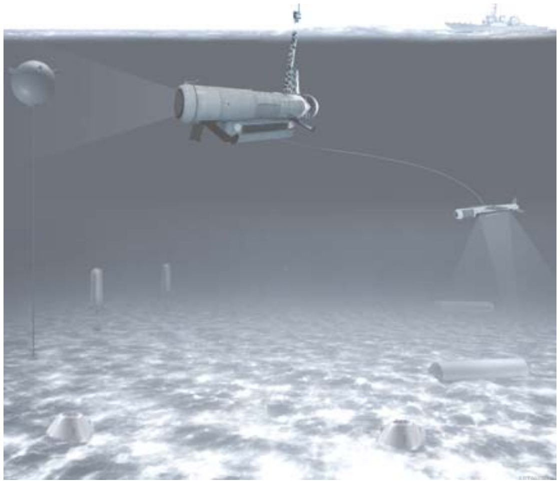

Fig. 1. Remote Minehunting System

The unmanned semi-submersible vehicle is being developed specifically to give carrier battle groups and amphibious-ready groups an organic mine reconnaissance capability in littoral waters.

Once launched from its host ship, the vehicle will use GPS coordinates to find its location, search area and track. To begin minehunting, the vehicle will deploy a towed variable depth sensor (VDS) designed to detect, localize, classify and identify moored and bottom mines. The sonar suite to be carried by the VDS can find mines with a high degree of probability at both deep and shallow coastal depths.

The RMV has a cylindrical body with a bottom-mounted pylon, which provides a streamlined cradle for the VDS when it is not deployed. A stern-mounted mast extends from the top of the RMV to provide an airway for the RMV's diesel engine. The mast also supports communication antennas and a collision-avoidance camera. Four anhedral fins extend from the RMV to provide control power in heave, roll, pitch and yaw. The RMV propulsor is encased with a stator / shroud assembly which improves efficiency while minimizing the roll torque imposed on the body.

C. RMV Simulation Overview

The Perry Technologies division of Lockheed Martin has a 24-year history of developing underwater vehicle simulations [1]. The WLD1 simulation is the latest evolution of these simulations, and is based on hydrodynamic coefficients derived from model testing [2]. The simulation also includes a coefficient-based representation of the AQS-20 towbody, the towbody autopilot control laws [3], and a dynamic cable model [4]. The dynamic representation of the vehicle is based on the methodology defined in Feldman [5]. These coefficients are specific to the WLD1 physical characteristics. The "at sea" tests were conducted with the Critical Item Test (CIT) prototype vehicle. This vehicle has significantly different physical characteristics from the WLD1 model. The main physical configuration differences are:

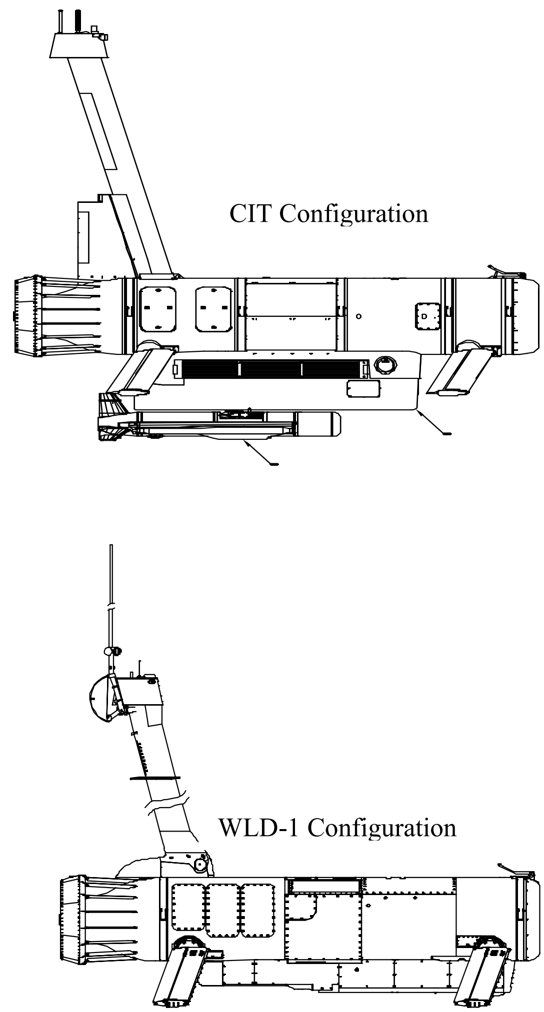

Fig. 2. CIT and WLD-1 Configurations

- The CIT vehicle has a larger pylon than the WLD1 vehicle, shorter in length but deeper.
- The CIT vehicle has a muffler section attached to the base of the snorkel.

Configuration differences must be accounted for in order to use CIT data for simulation validation. Figure 2 shows a comparison of the vehicles. This paper documents the process used to quantify the configuration differences in terms of hydrodynamic coefficients. It then goes on to compare the adjusted (for CIT configuration) simulation with the latest data collected during "at sea" testing.

D. Adjustments to Coefficients

The significant differences between the WLD-1 and CIT vehicles were primarily in the shapes and sizes of vertically mounted appendages. Since these appendages would be primarily affected by flow in the lateral direction, only the lateral plane (Sway, Roll and Yaw) coefficients were adjusted. For example, to see the effect of the larger CIT pylon on Yv' (normalized sway force change with respect to sideslip angle) we need to get Yv' in terms of the area and lift coefficient of the pylon. Then, starting with the base Yv' (Yv' of the entire vehicle), subtract off the Yv' due to the WLD1 pylon, and add the Yv' due to the CIT pylon.

Assume the appendage such as a mast; muffler, or pylon acts as a lifting surface (see figure 3).

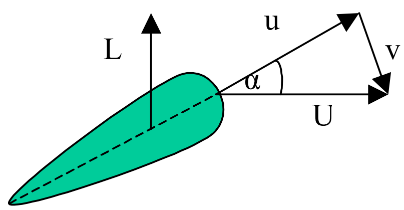

Fig. 3. Lifting Body Approach for Modifying Coefficients

For small α

$$\alpha = \tan\frac{v}{u} \cong \frac{v}{u} = v'$$

For small α ≅ U

Assume the lift coefficient is proportional to the local angle of attack (Note: C_l is the opposite sign of v')

$$C_l = -k\alpha(rad) \cong -kv' \qquad (1)$$

Then lift becomes

$$L = -\frac{1}{2}\rho A k v' U^2 \qquad (2)$$

Normalizing the lift force in the standard manner (dividing by $\frac{1}{2}\rho l^2 u^2$) yields,

$$L' = \frac{-Akv'}{l^2} \qquad (3)$$

For appendages such as a mast, muffler or pylon, which are vertically mounted, u is the forward velocity, v is the sideslip velocity and the lift is a Y (sway) force.

Hence for any vertically mounted appendages we can express the derivatives as follows:

Starting with equation (3) , and substituting Y' for L', taking the derivative w.r.t. v' gives the local coefficient Y_v'

$$Y'_v = \frac{-Ak}{l^2} \qquad (4)$$

The relationship between the locally generated, normalized sway force and the resulting normalized roll torque felt by the body is:

$$K' = -Y' * \left(\frac{z_{cp}}{l}\right) \qquad (5)$$

Combining equations 4 and 5 gives the local coefficient of normalized roll with respect to sideslip, K_v'

$$K'_v = \frac{Akz_{cp}}{l^3} \qquad (6)$$

N_v' is calculated in a similar manner. For rotary motions, the local sideslip velocity is calculated by multiplying the angular velocity by the appropriate offset distance. Table 1 summarizes the effects of vertical "wing like" appendages on the body coefficients.

TABLE I

COEFFICIENT ADJUSTMENTS FOR AN APPENDAGE

	v'	ρ'	r'
Y'	$\frac{-Ak}{l^2}$	$\frac{Akz_{cp}}{l^3}$	$\frac{-Akx_{cp}}{l^3}$
K'	$\frac{Akz_{cp}}{l^3}$	$\frac{-Ak(z_{cp})^2}{l^4}$	$\frac{Akx_{cp}z_{cp}}{l^4}$
N'	$\frac{-Akx_{cp}}{l^3}$	$\frac{Akx_{cp}Z_{cp}}{l^4}$	$\frac{-Ak(x_{cp})^2}{l^4}$

Where:

A= Lift area of the appendage.

k= Multiplier that relates lift coefficient (C_l) to angle of attack (α).

x_{cp} = x distance from C.G. of vehicle to C.P. of appendage.

z_{cp} = z distance from C.G. of vehicle to C.P. of appendage.

L= length of vehicle.

Using the above formulas the vehicles coefficients can be adjusted for differences in the mast, muffler, and pylon. The base CIT horizontal plane coefficients can be calculated from the WLD1 base coefficients by subtracting the WLD1 appendage and adding the CIT appendages. For example the CIT Y_v base coefficient can be calculated as follows:

$$Y'_{vCITbase} = Y'_{vWLD1base} - Y'_{vWLD1pylon} + Y'_{vCITpylon} - Y'_{vWLD1mast} + Y'_{vCITmast} + Y'_{vCITmuffler} - Y'_{vWLD1aftfin} + Y'_{vCITaftfin} \quad (7)$$

E. Validation of Lateral Plane Coefficients

We need to now compare the simulation with the new adjusted horizontal plane coefficients to data taken during the CIT2c test. Steady turning data was used to make two comparisons. The first is roll torque induced by yaw rate, and the second is yaw torque required to develop yaw rate. Note that the "measured" roll and yaw torque is actually the requested control torque that gets converted to fin angle. Figures 4 and 5 show the comparison of simulation results to CIT data. It can be seen that the slope of the Yaw Torque prediction was within 3% of the data. The small offset of Yaw Torque at 0 turn rate is due to small misalignments of the appendages and wings in the prototype vehicle. The Roll Torque slope of the simulation was within 25% of the data. Analysis shows that this slope is very sensitive to the wing shadowing effects and the pylon lift slope, which are two of the most uncertain parameter estimates used in the corrections.

The Roll and Yaw Torque slopes can be analytically predicted as follows.

$$-K'_c = \left[K'_r - \frac{K'_v \left(Y'_r - m' \right)}{Y'_v} \right] r' \quad (8)$$

$$-N'_c = \left[N'_r - \frac{N'_v \left(Y'_r - m' \right)}{Y'_v} \right] r' \quad (9)$$

The slopes predicted by equations (8) and (9) are $K'_{cr} = -.013$ and $N'_{cr} = .037$. The large difference between the analytical estimates and the simulation is used by the control system to position the control surfaces. It was found that these algorithms overestimated the v and w components of the free stream velocity vector that the wings encounter. When the simulation is rerun using improved wing-positioning algorithms, N'_{cr} matches within 1%.

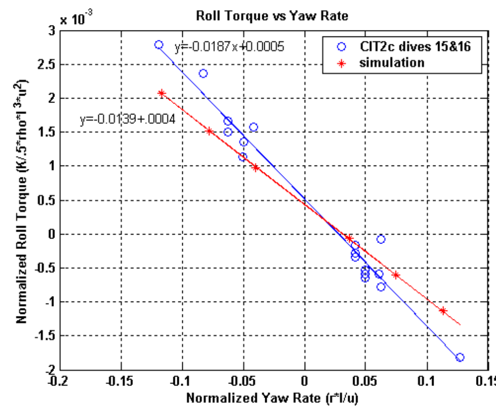

Fig. 4. Comparison of Simulation and Vehicle Data for Roll During Turns

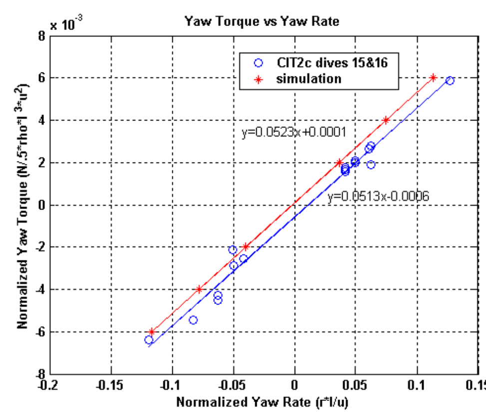

Fig. 5. Comparison of Simulation and Vehicle Data for Yaw During Turns

F. Vertical Plane Validation

Vertical plane forces (Heave and Pitch) are the result of three significant factors – Hydrodynamic forces, static buoyancy effects and near-surface suction forces. The body hydrodynamics are nominally well understood, due to extensive scale model tests on the WLD-1 body. The CIT body should be very similar, but affects like increased pylon drag cause some uncertainty. Additionally, small misalignment in the control surfaces will cause some uncertainty in the steady hydrodynamic forces. Static effects are well understood. The most difficult effect to quantify analytically is the near-surface suction effect. This effect is small in comparison to the steady hydrodynamic forces when the vehicle is at operating depth, but the rate of change of theses forces as the vehicle approaches the surface can have a strong destabilizing effect on the vehicle [6]. An attempt was made to fit an estimate of the surface suction forces based on at-sea data. Figure 6 shows that the simulation with the updated near-surface effects provides a good match for the at-sea data

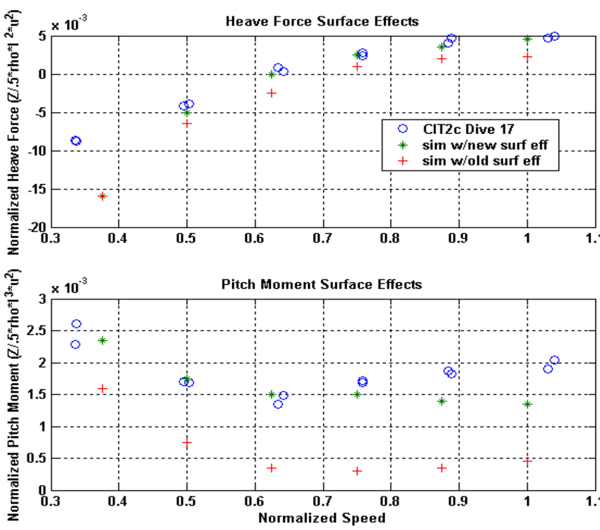

Fig. 6. Simulation Comparisons with CIT2c Speed Sweep

G. Step Responses

The dynamic response of the simulation was compared to CIT2c data performing steps in each of the control loops. Figures 7-10 show a comparison of roll, depth, pitch, and yaw step responses. Note that the data was obtained in the open ocean with significant wave action. Statistically comparable sea states were input to the simulation, but random wave motion cannot be duplicated exactly.

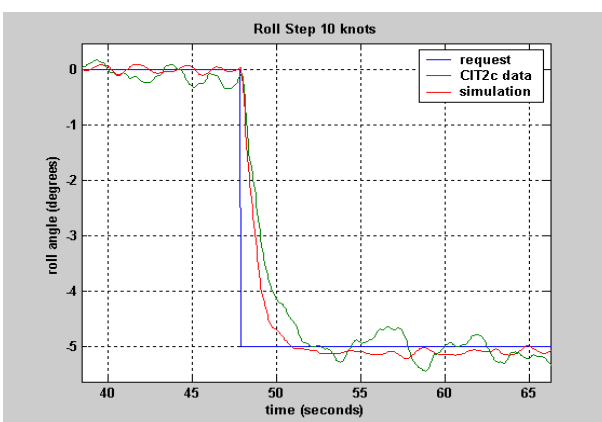

Fig. 7. Roll Step Response Comparison

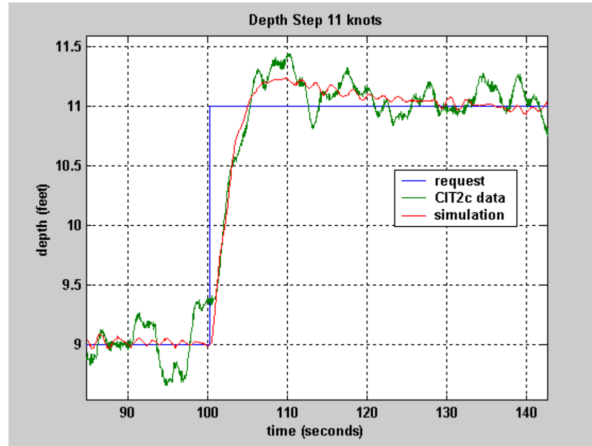

Fig. 8. Depth Step Response Comparison

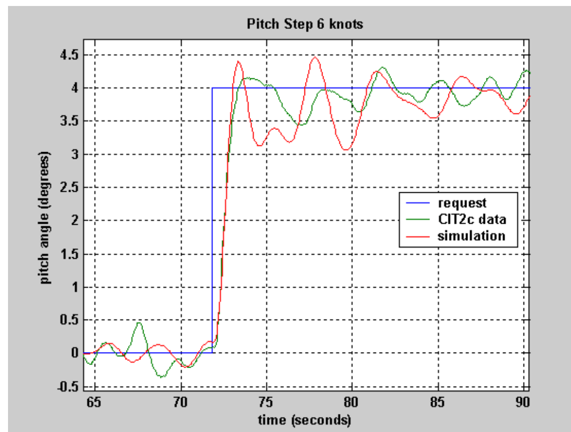

Fig. 9. Pitch Step Response Comparison

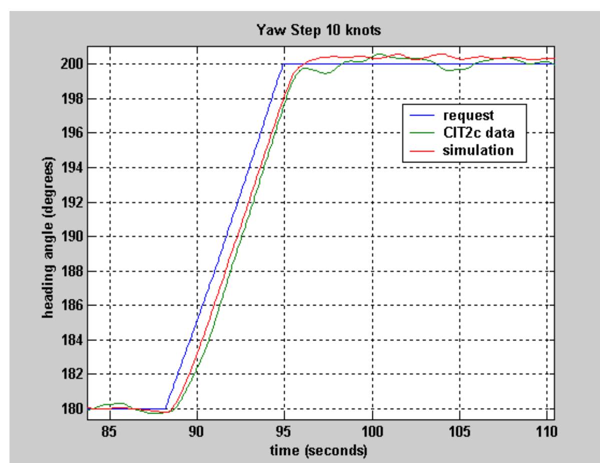

Fig. 10. Yaw Step Response Comparison

II. CONCLUSION

A high fidelity simulation of the AN/WLD-1 Remote Minehunting vehicle has been created. The validation of this simulation was performed on a prototype vehicle with small but significant modification to the vehicles body. Analytical adjustments to the hydrodynamic coefficients obtained from scale model testing were used to make the simulation match the prototype test vehicle. These adjustments were based on vehicle configuration differences, not just empirical "tweaks" to match the at-sea data. Simulation results using the adjusted coefficients gave good matches to the at-sea data. High confidence has been gained in the ability of the WLD-1 system to meet its operational requirements and transition into service.

References

[1] Rushfeldt, P "Control System and HydroDynamic Analysis for TUMS (Turbo Unmanned Submersible)", 1984 Offshore Technology Conference, May, 1984

[2] Barr, R, "Model Tests Of The Remote Minehunting Vehicle", Hydronautics, Inc. Report, August 2001

[3] Kueny, K, "AQS-20x Autopilot DLL Letter Report", Vehicle Control Technologies, Inc. Report, March 2001

[4] Radanovic, B. and Driscoll, R., "Development Of A General Purpose Cable Model And Simulation For Marine Applications", Oceans2002, October, 2002

[5] Feldman, J, "DTNSRDC Revised Standard Submarine Equations of Motion", Report DTNSRDC/SPD-0393-09, June 1979

[6] Larkin, L, Thomsen, C, Feldman, J. "Dynamics Of A High Speed Autonomous Semisubmersible Vehicle", Oceans2002, October, 2002